



HAL
open science

Impact of high frequency current ripples on the degradation of high-temperature PEM fuel cells (HT-PEMFC)

Thomas Jarry, Amine Jaafar, Christophe Turpin, Fabien Lacressonniere, Eric Bru, Olivier Rallieres, Marion Scohy

► To cite this version:

Thomas Jarry, Amine Jaafar, Christophe Turpin, Fabien Lacressonniere, Eric Bru, et al.. Impact of high frequency current ripples on the degradation of high-temperature PEM fuel cells (HT-PEMFC). International Journal of Hydrogen Energy, 2023, 10.1016/j.ijhydene.2023.03.027 . hal-04042863

HAL Id: hal-04042863

<https://ut3-toulouseinp.hal.science/hal-04042863>

Submitted on 23 Mar 2023

HAL is a multi-disciplinary open access archive for the deposit and dissemination of scientific research documents, whether they are published or not. The documents may come from teaching and research institutions in France or abroad, or from public or private research centers.

L'archive ouverte pluridisciplinaire **HAL**, est destinée au dépôt et à la diffusion de documents scientifiques de niveau recherche, publiés ou non, émanant des établissements d'enseignement et de recherche français ou étrangers, des laboratoires publics ou privés.

Impact of high frequency current ripples on the degradation of high-temperature PEM fuel cells (HT-PEMFC)

Thomas JARRY^{a,*}, Amine JAAFAR^a, Christophe TURPIN^a, Fabien LACRESSONNIERE^a, Eric BRU^a,
Olivier RALLIERES^a, Marion SCOHY^b

^a LAPLACE, Université de Toulouse, CNRS, Toulouse INP, UPS, Toulouse, France

^b Safran Power Units, F-31707 Toulouse, France

* Corresponding author. Tel.: +33 5 34 32 23 56.

E-mail address: thomas.jarry@laplace.univ-tlse.fr (T. Jarry).

HIGHLIGHTS

- Two HT-PEMFC single cells are operated for 2 600 h at 0.2 A/cm² with 20 kHz 20 %_{pp} triangular current waveform.
- Ageing is compared with two HT-PEMFC single cells operated simultaneously at the same constant mean current density.
- Evolution of the cells voltages during the endurance and characterization phases is similar with and without HF current ripples.
- Reduction of ECSA leading to an increase in activation losses is found for all tested fuel cells.

ABSTRACT

In order to achieve the goal of reducing the environmental footprint of the transport sector, new low-carbon energy systems including fuel cells and power converters are proposed. The sizing and operation of such systems have to take into account the aging of the fuel cell. This paper focuses on the study of a potential impact of high frequency current ripples (HFRCR) on the degradation of a high-temperature proton exchange membrane fuel cell (HT-PEMFC). A 2 600 h long endurance test was carried out on 4 HT-PEMFC single cells with and without HFRCR. The degradation of two cells operated with a triangular current waveform of frequency 20 kHz and amplitude 20 %_{pp} of the mean current density (0.2 A/cm²) is compared to the degradation of two cells operated at the same constant mean current density. In addition to endurance phase, several characterization phases (polarization curves, electrochemical impedance spectroscopy and cyclic voltammetry) are used to analyse the impact of the current harmonics. The obtained results show that the high frequency current ripples do not seem to accelerate the degradation of the HT-PEMFC single cells.

Keywords: Current harmonics, HT-PEMFC, Single cell, Aging, Power converter, Hydrogen.

1. Introduction

The need to strongly reduce greenhouse gas emissions to minimize the global warming leads to develop and use low-carbon energy systems. Fuel cells are a technology that can contribute to reach this goal. Indeed, a fuel cell produces electricity, heat and water from hydrogen and oxygen. As this technology is quiet, non-polluting and capable of using hydrogen or other fuels produced from renewable sources, it appears to be a promising solution. Among the fuel cell technologies, the high temperature proton exchange membrane fuel cell (HT-PEMFC) operates at 160 °C and presents some advantages: the heat produced is more easily recoverable and the cooling system is more compact compared to the low temperature proton exchange membrane fuel cell (LT-PEMFC). The high temperature of operation also increases the tolerance to impurities such as carbon monoxide or hydrogen sulfur [1]. In addition, the use of a polymer membrane soaked in phosphoric acid eliminates the need for a gas humidification system. These advantages allow to reduce the size of the fuel cell balance of

plant (BOP), facilitate the use of reformed hydrogen and allows multi-generation on-board: electricity, heat and water [2], which is interesting for embedded applications. However, today, this technology presents a lower specific power and performance than the LT-PEMFC technology and still exhibits too rapid aging especially in embedded applications [1], two crippling obstacles in the context of such applications.

Fuel cell systems are most often connected to a power converter in order to deliver a direct current (DC) or alternative current (AC) bus. In addition, to optimize the sizing of the fuel cell for embedded applications, the fuel cell is often hybridized with at least one power source through power converters that also allow to regulate the operating point of each sources [3]. However, by operating principle, power converters induce current ripples on the fuel cell current, whose frequency and amplitude depend on the topology and control of the power converters [4]. The most common power converters topologies connected to a fuel cell and the current waveform produced by their operation are shown in Fig. 1. Passive and active filters may be used to reduce the amplitude of the fuel cell current ripples, both for high frequency (HF) and low frequency (LF) current harmonics. However, their utilisation increases the mass, volume, power losses and cost of the system [5].

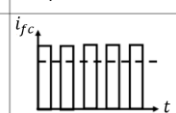
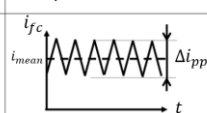
Converter	DC/DC buck converter	DC/DC boost converter	DC/AC inverter
Current waveform (without filter)			
f_{ripple}	HF few kHz to 100+ kHz	HF few kHz to 100+ kHz	HF + LF few kHz to 100+ kHz + 100-120 Hz
Δi_{pp}	200 % _{pp} of i_{mean}	10-20 % _{pp} of i_{mean}	400 % _{pp} of i_{mean}

Fig. 1: Several fuel cell current waveforms according to power converters topologies.

It is progressively affirmed, for the LT-PEMFC, that low frequency current ripples (LFCR), lower than a range between 0.1 and 1 kHz, have a negative impact on the efficiency (power losses [6]) and the aging of the fuel cells. For the lowest frequencies, the degradation is especially caused by the possible lack of reactant gas flows, that must follow the current ripples. Depending on their frequency and the dynamic of fuel cell BOP

(e.g. the air compressor), LFCR can lead to a gas starvation phenomenon which affects the aging mechanism in the fuel cell [7, 8]. LFCR also generate mechanic stresses (variation of the pressure due to variation of gas flows) and thermal cycling [8]. The aging behaviour of LT-PEMFC supplying a current with LFCR has been studied in [8–10]. Some authors also study means to reduce LFCR amplitude through new converter topology or control [5].

In the case of high frequency current ripples (HFCR), the electric double-layer phenomenon, consisting in the storage of electric charges at both electrode-membrane interfaces, acts as a low-pass filter for the main reaction [11]. For frequencies above 1 to 10 kHz, current ripples are nearly totally absorbed and supplied by the charges stored at these electrode-membrane interfaces, while the main fuel cell reaction is governed by the mean current. While the HFCR do not lead to an increase in activation and diffusion losses, they increase the ohmic losses [11].

In order to understand the aging behaviour of the electrodes and/or the membrane caused by the HFCR, some studies are carried out only for LT-PEMFC. In almost all publications, the behaviour of a stack is studied by comparing the aging effects according to different currents having the same mean value : a constant current and a current with HFCR [12–16]. In [12], the current waveform applied is a single harmonic of 1 kHz with a peak-to-peak amplitude of 10 %_{pp} of the mean current value (250 A). During a 1 000 h endurance test, the voltage of the 5-cell stack with HFCR degrades 10 % faster than the stack without HFCR. Characterizations (polarization curve, electrochemical impedance spectroscopy (EIS)) are regularly performed during the test. They also show a stronger degradation of the stack with HFCR, which presents increased activation and diffusion losses. On the contrary, in [13, 14], the aging of a 5-cell stack with a 5 kHz triangular current waveform with an amplitude of 20 %_{pp} at 0.5 A/cm² mean current value leads to a lower degradation of the polarization curves than the stack without HFCR. However, the voltage of the stack with HFCR degrades faster during endurance, thus the presence of reversible losses is suspected. The accumulation of reversible losses during endurance and their recovery during the characterization phases is clearly shown in [15] and attributed to a possibly more difficult water management in LT-PEMFC operated with HFCR. At variance, a 5-cell stack operated with a 5 kHz triangular current waveform with an amplitude of 20 %_{pp} of 0.7 A/cm² mean current value degrades slower during endurance than the stack without HFCR, but faster when the polarization curves are compared [16]. These contradictory results raise the importance of the reproducibility of these endurance tests. Finally, the evolution of the electrochemical surface area (ECSA) has been studied for LT-PEMFC single cells operated in H₂/N₂ with and without voltage ripples between 0.6 and 0.9 V at different frequencies (1 Hz to 1 kHz) [10]. The comparison with a single cell operated at the same mean voltage value of 0.75 V (and not the same mean current value in this case) after 51 h of endurance test shows no difference in ECSA evolution for the 1 kHz current ripples.

In the case of HT-PEMFC, the higher operating temperature, the simplification of the water management (no gas humidification) and the use of phosphoric acid may have an impact on the degradation of the fuel cell in presence of HFCR. Common degradation mechanisms in HT-PEMFC include acid loss, Pt-particle growth and carbon corrosion [1,17,18].

The objective of this paper is to present the results of a 2 600 h long endurance test performed on two HT-PEMFC single cells operated with a 20 kHz triangular current waveform with an amplitude of 20 %_{pp} of the 0.2 A/cm² mean current

density value. Two other single cells are operated on the same test bench with a constant current of 0.2 A/cm². After a brief description of the test bench and the single cells used for this endurance test in section 2, the results obtained for both during endurance and characterization phases will be presented in section 3. Main conclusions and perspectives are summarized in section 4.

2. Endurance tests

2.1. Experimental test bench

The test bench used for the endurance tests is able to operate with 4 HT-PEMFC single cells operated in H₂/air disposed in series on two power circuits. A simplified diagram is presented in Fig. 2. Each power circuit is composed of low inductance cables, DC contactor, current probes and a high-speed active load (Kikusui PLZ334WL) able to perform current slopes up to 50 A/ μ s. The serial connection of the two single cells is done through bus bars to minimize the serial inductance value. An illustrated picture of the power circuits is given in Fig. 3.

The cells are operated at atmospheric pressure. In order to avoid the impact of atmospheric pressure variation on the cells' voltages during the aging tests, it is interesting to be able to compare, at the same time, the aging mechanism of fuel cells on different power profiles. Indeed, the atmospheric pressure variation has a non-negligible impact on the performances [19]. The inlet and outlet pressure of each single cell compartment is measured. Each fluidic outlet passes through a purger to separate gas and liquid fractions. Then, the hydrogen outlets of the two cells of each power circuit are connected together (as shown in Fig. 2). It is the same for the air outlet in order to separate the operation of the two circuits as much as possible.

The regulation of the gas flows is done with mass flow controllers and based on the measurement of the currents on each power circuits, with stoichiometry values of 1.2 for H₂ and 2 for air. The temperature of each fuel cell is regulated with resistive plates placed on the terminal plates of each single cell and with fans blowing on these terminal plates. The operating temperature is 160 °C, with a +/- 0.5 °C variation during endurance phase, and +/- 1.5 °C at most during characterization phase. Finally, nitrogen is used at both electrodes for start-up and shut-down sequences to limit the degradation associated with H₂ and O₂ presence at the same time at the anode [20]. To limit the degradation, resistors of 0.22 Ω are used for each single cells in order to limit their operation at high cell voltages (i.e. above 0.8 V) [21].

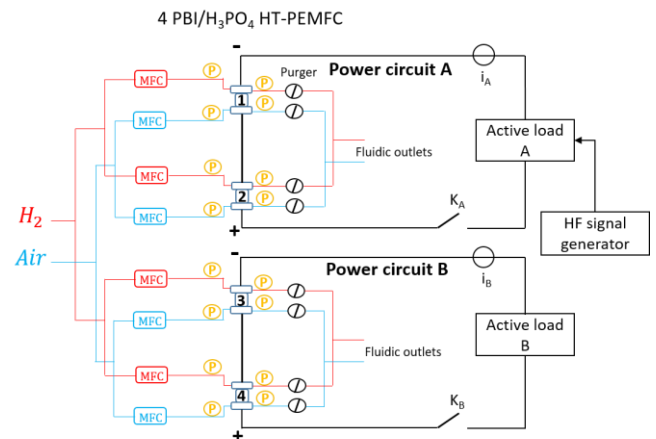


Fig. 2: Simplified diagram of the test bench.

2.2. HT-PEMFC single cells

The tested single cells are PBI/H₃PO₄ HT-PEMFC made by the company ADVENT TECHNOLOGIES and visible in Fig. 3.

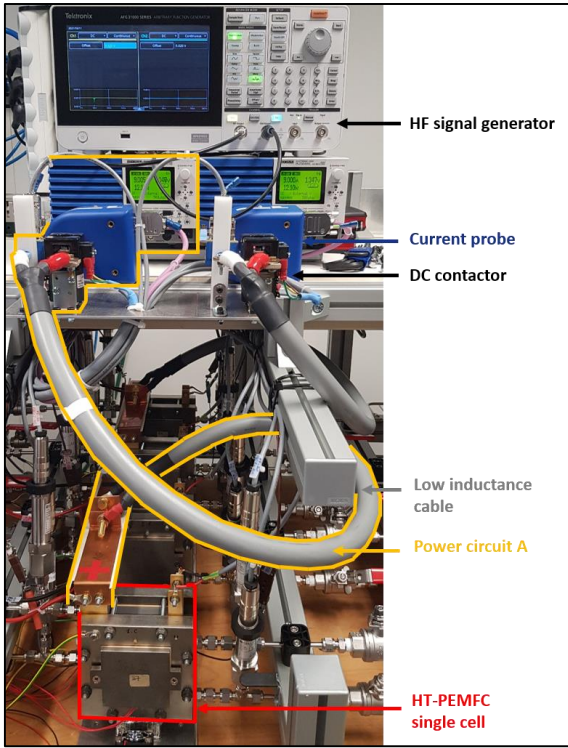


Fig. 3: Power circuit of experimental test bench.

They have an electrode surface of approximately 45 cm² and a membrane-electrode assembly (MEA) 900 μm thick, with an approximately 80 μm thick membrane. The MEA and the other components of the single cells (terminal, current collector and flow plates, O-rings, gaskets) are received separately and mounted in the laboratory. Leak tests are carried out with nitrogen at 120 °C before the breaking-in phase consisting of a 14-hours long operation in H₂/air at 0.2 A/cm² and 180 °C.

2.3. Characterization phase

Before endurance tests, an initial characterization is carried out with different phases:

- Cyclic voltammetry in H₂/N₂ at 160 °C with voltage variation 30 - 800 mV at 50 mV/s. The gas flows values are equivalent to an operation of the fuel cell at 0.05 A/cm² with stoichiometry values of 1.2/2.
- Polarization curve with EIS with regulated gas flows.
- Polarization curve with EIS at constant maximum gas flows (equivalent to an operation of the fuel cell at 1.22 A/cm² with stoichiometry values of 1.2/2).
- Large current sweepings 0 - 1.1 A/cm² at different frequencies: 100 mHz, 500 mHz, 1 Hz and 10 Hz. They need to be performed at constant maximum gas flows (equivalent to 1.22 A/cm²) because of gas flow regulation limitations.

This characterization phase is also used to identify both a quasi-static and a dynamic model of the HT-PEMFC single cell.

The quasi-static cell voltage model (U_{fc}) is given by equation (1) and is constituted by a voltage source representing the reversible Nernst voltage E_{rev} (2) in series with two variable current sources modelling activation and diffusion voltage drops, respectively η_{act} (3) and η_{diff} (4) [22]. The value of E_{rev} for a fuel cell working in H₂/Air at a temperature of 160 °C (T_{fc}) is given in Table 1. The current source i_n notably represents the effect of the parasitic reactions and of the crossover of active gases through the membrane on the fuel cell voltage. Ohmic losses are represented by the resistor R_{ohm} . The

signification of the parameters along with their values (for cell 1) are given in Table 1.

$$U_{fc} = E_{rev} - \eta_{act} - \eta_{diff} - R_{ohm} * i_{fc} \quad (1)$$

$$E_{rev} = \frac{T_{fc} \Delta S^0}{nF} - \frac{\Delta H^0}{nF} + \frac{RT_{fc}}{nF} \ln \left(\frac{p_{H_2} (p_{O_2})^{1/2}}{p_{H_2O}} \right) \quad (2)$$

$$\eta_{act} \approx \frac{RT_{fc}}{\alpha nF} \ln \left(\frac{i_{fc} + i_n}{i_0} \right) \quad (3)$$

$$\eta_{diff} = - \frac{RT_{fc}}{\beta nF} \ln \left(1 - \frac{i_{fc} + i_n}{i_{lim}} \right) \quad (4)$$

The dynamic model is shown in Fig. 4. It is an equivalent circuit based on the quasi-static model, with two capacitors noted respectively C_{dc} and C_{diff} . They allow to take into account the double-layer phenomenon and the gas diffusion dynamics [11,21,22].

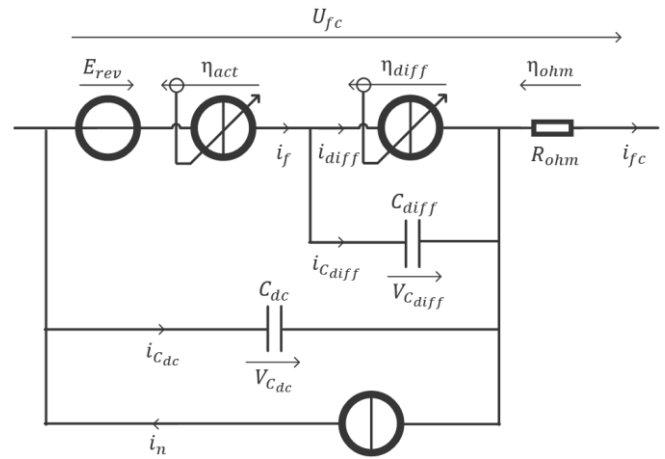


Fig. 4 : Equivalent circuit dynamic model of the HT-PEMFC single cell.

The polarization curve with regulated gas flows is used to identify the parameters of the quasi-static model. R_{ohm} is measured with EIS at high frequency (typically 5 to 10 kHz). The example of the identification of a polarization curve (for cell 1 with regulated gas flows, before endurance test) is given in Fig. 5. The obtained parameters are given in Table 1. The quasi-static model allows to separate the activation, diffusion and ohmic losses. Their evolution with the fuel cell current is also visible in Fig. 5. This is used later in this paper (Fig. 9) to study the evolution of activation, diffusion and ohmic losses with the current density before and after the aging test.

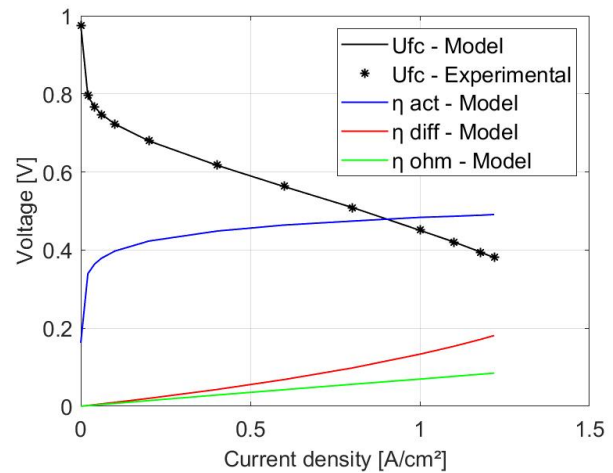


Fig. 5 : Identification of the quasi-static model with an experimental polarization curve.

Table 1 : Parameters of the quasi-static model for a 45.2 cm² fuel cell.

Parameter	Designation	Value
E_{rev}	Reversible cell voltage	1.206 V (calculated)
α	Charge transfer coefficient	0.5 (fixed)
i_0	Exchange current	9.7E-05 A (identified)
β_{diff}	Diffusion factor	0.14 (identified)
i_{lim}	Diffusion limit current	73.7 A (identified)
i_n	Internal current	7.4E-03 A (identified)
R_{ohm}	Total ohmic resistance	1.6E-03 Ω (measured with EIS)

For the dynamic model, the current sweepings are used to identify the values of C_{dc} and C_{diff} . To enhance the precision of this identification, the quasi-static parameters obtained previously with the polarization curve are used during this second phase identification.

In the work presented in this paper, only the fuel cell quasi-static model is used. However, we have presented the full characterization process, including current sweepings and polarization curve at maximum gas flows that are used to identify the parameters of the fuel cell dynamic model, as it could be degrading for the fuel cell.

2.4. Test configuration

After the characterization phase, the single cells are operated at the same mean current value of 0.2 A/cm², the cells 1 & 2 (power circuit A) producing a triangular current waveform with frequency and amplitude of respectively 20 kHz and 20 %_{pp} values.

In Fig. 6, the cell voltage measured at the terminal of the cell 1 is presented when the cell operates with a triangular current waveform. As one can see, the cell undergoes large variation voltage with the same frequency as the current. The voltage magnitude is only due to ohmic losses [11] and the total ohmic resistance (R_{ohm}) can be estimated from the magnitude measurements (ΔU_{fc} and Δi_{fc}). Hence, we have obtained a total ohmic resistance value approximately equal to 1.5 m Ω , close to ohmic values found with EIS. Indeed, as one can see on the equivalent circuit dynamic model, for high frequency current solicitations, the double-layer capacitor C_{dc} acts as a filter and the dynamic components of i_{fc} only pass through the resistor R_{ohm} .

Cells 3 & 4 (power circuit B) are operated at constant current (Fig. 6).

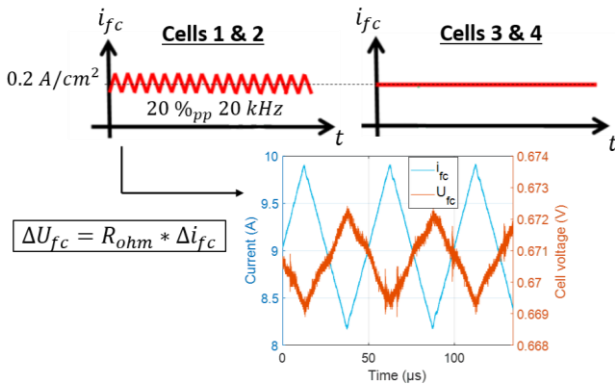


Fig. 6: Current waveforms and cell voltage (for the cell 1) measured during the test configuration.

3. Analysis of the aging test

3.1. Analysis exploiting endurance phase

The evolution of the voltage of the 4 cells relatively to their initial voltage is presented in Fig. 7.

Two events led to the shut-down of the test bench during the endurance test:

- After 1 000 h of endurance, the closure of the laboratory has led to a controlled shut-down for 3 weeks, with characterizations (same as the initial one but without cyclic voltammetry) made before and after the closure and respectively called “intermediate 1” and “intermediate 2”.
- After 2 300 h of endurance, the failure of a component led to an emergency shut-down of the cells. Because of the parallelization of the gas inlets and inevitable differences in pressure drops between the cells, the flow of nitrogen used to purge the cells has not been equally distributed among the 4 cells, which seems to have led to an uneven degradation of the cells as visible in Fig. 7.

While some differences in the voltage evolution during endurance are observed between the 4 cells, the presence of the HFCR do not seem to lead to a faster degradation: no important differences are observed between the two power circuits. The cells present an average voltage drop value of 10 μ V/h before the controlled shut-down and of 5 μ V/h after (once the voltages are stabilized after restarting). These voltage drop values are in the same order of magnitude of values found in the literature for HT-PEMFC operated at constant current [23–26].

The evolution of the pressure drop on the air outlet side of the 4 cells is also presented in Fig. 7. After 1 700 h of the endurance test, the pressure drop of cells 3 & 4 increase, probably due to a water or an acid plug. Another interesting observation, which may be related to the first one, is the reversible voltage loss observed on cell 4 after 2 100 h, which is recovered after the emergency shut-down. As the other parameters (pressure, temperature, gas flows) of the cell stay constant, this loss could be linked to an acid loss from the cell, due to acid redistribution inside the cell. These phenomena are only observed for the cells without HFCR. No impact of the presence of HFCR is visible on the evolution of the cell voltages of the single cells. We thus seek to exploit the characterization phases to identify a potential impact of the current harmonics.

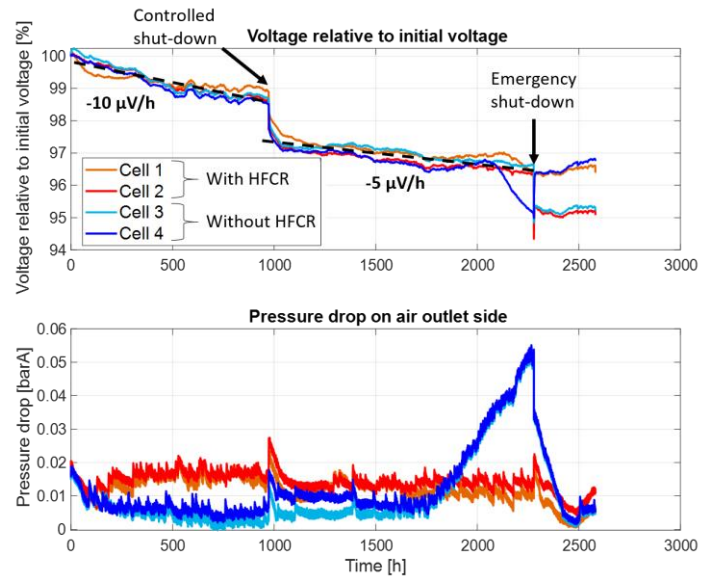


Fig. 7: Evolution of the cell voltage (top) and the pressure drop at air outlet (down) during the endurance test.

A final characterization is performed after 2 600 h. As it is done after the emergency shut-down, it does not seem very relevant to exploit this characterization (we will however compare the cyclic voltammetry performed during initial and final characterizations).

The comparison of initial and intermediate (before and after the controlled shut-down) characterizations will now be presented.

3.2. Analysis exploiting intermediate characterization phases after 1 000 h of endurance

The voltage difference between the initial and the first (“intermediate 1”) or the second (“intermediate 2”) intermediate characterizations for each step of the polarization curve (with regulated gas flows) is presented in Fig. 8a. During the first intermediate polarization curve, an experimental error on the gas flow rates has led to the measure of the voltages for two current density values (0.04 and 0.05 A/cm²) at higher stoichiometry values (wrong points circled in red in Fig. 8).

Globally, the voltage evolution of the 4 cells between the initial and the intermediate polarization curves is similar, although the cells 3 & 4 seem slightly more degraded at high currents and also for the second intermediate characterization. The difference between the first and second intermediate polarization curves may be attributed to:

- A degradation due to both the shut-down and start-up of the cells and the impact of the characterization phase.
- Internal changes in the MEA during the 3 weeks of closure such as acid redistribution.

The evolution of the voltage difference with the current density, which may be called the “signature” of the quasi-static degradation of the cells, allows to know which type of phenomenon is at the origin of cell degradation: increase of activation, diffusion and/or ohmic losses [29]. An increase in activation losses, due to a decrease of the ECSA, leads to a constant voltage difference with the current density (except at very low values of current densities). An increase in diffusion losses, due to a degradation of gas transport conditions in the MEA, leads to a logarithmic or nearly linear evolution of voltage difference with the current density. Since an increase in ohmic losses also leads to a linear evolution of voltage difference with the current density, it is interesting to subtract the ohmic losses (to obtain IR-free polarization curve) in order to see only the evolution of activation and diffusion losses. This is done thanks to the measurement of R_{ohm} (by EIS) during the characterizations. While a slight increase in total ohmic resistance value is found for all the cells during endurance test, no effect of the HFCR on its evolution can be observed.

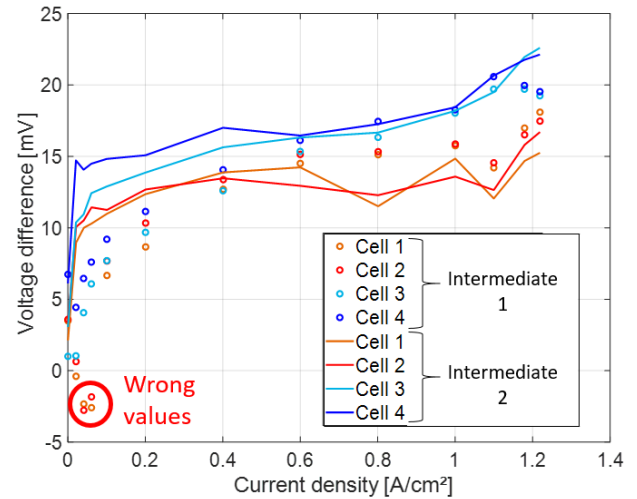
The voltage difference between initial and intermediates IR-free polarization curves is presented in Fig. 8b. The removal of the ohmic losses does not change the “signature” of the quasi-static degradation of the cells, which seems due to an increase of both activation and diffusion losses. Cells 3 & 4 seem to present a slightly higher increase of diffusion losses, mainly visible at high current densities and for the second intermediate characterization.

An additional analysis of the degradation can be led from the quasi-static model. The initial and the second intermediate polarization curves are used to identify the model parameters. Hence, the evolution of activation, diffusion and ohmic losses with the current density can be drawn, as illustrated for cell 1 in Fig. 9. As you can see, the quasi-static model mainly explains the degradation of all single cells by an increase of the activation losses.

The analysis of initial and intermediate characterizations (after 1 000 h of endurance) does not make it possible to

distinguish a specific impact of the HFCR on the degradation of the single cells.

a) Voltage evolution between initial and intermediate characterizations



b) IR-free Voltage evolution between initial and intermediate characterizations

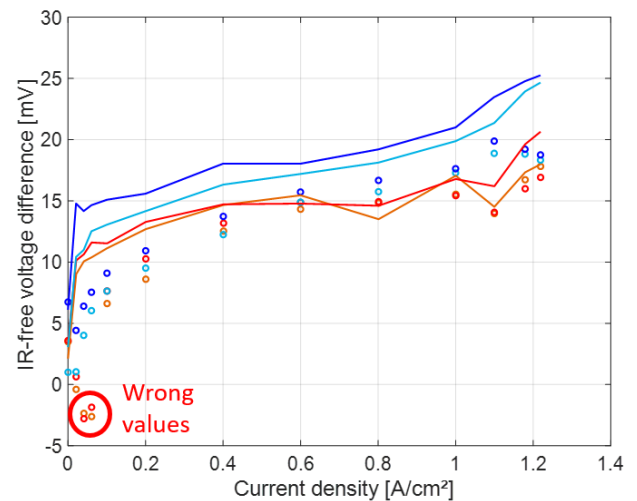


Fig. 8: Voltage difference between the initial and the first or the second intermediate polarization curves, with ohmic losses (a) or without (b).

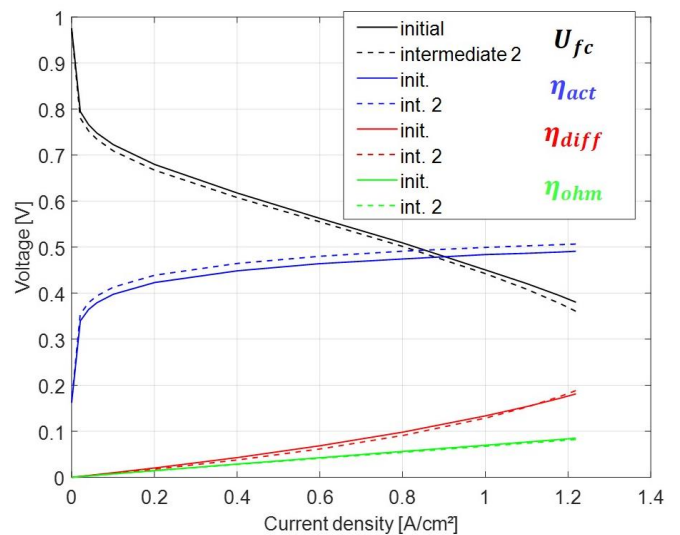


Fig. 9: Modelling of activation (blue), diffusion (red) and ohmic (green) losses for the initial and the “intermediate 2” polarization curves for cell 1.

3.3. Analysis exploiting cyclic voltammetry performed in initial and final characterization phases

The results of the cyclic voltammetry performed during initial and final characterizations (after 2 600 h of endurance) are presented in Fig. 10. Cyclic voltammograms are typically used to estimate the ECSA, the electrochemical double-layer capacitor value and the gas crossover value. In HT-PEMFC, the use of phosphoric acid leads to the presence of $H_2PO_4^-$ ions that are absorbed on the Pt and thus influence the quantitative estimation of the ECSA [30]. However, the qualitative comparison of the area under the peak (orange arrow in Fig. 9) between initial and final characterizations can be used to estimate the evolution of ECSA.

A degradation of ECSA is observed for all four cells, which is consistent with the increase in activation losses found in section 3.2. While some cells seem more impacted than others, no specific impact of the HFRCR on the evolution of ECSA is found.

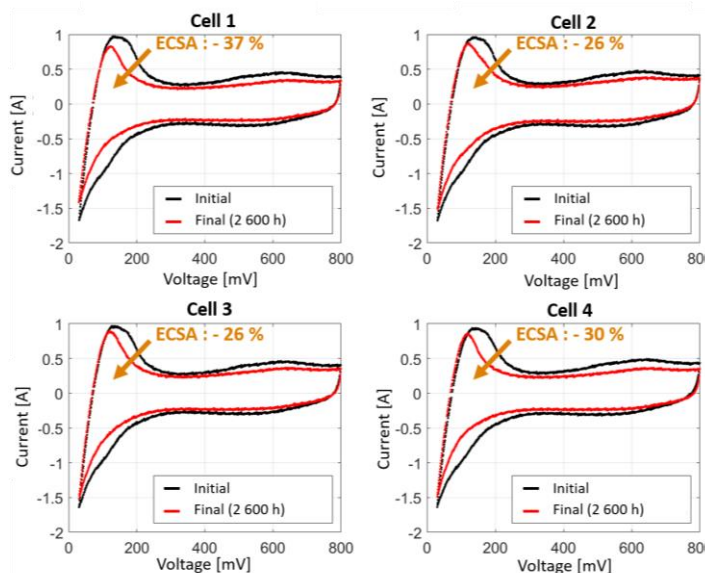


Fig. 10 : Cycling voltammograms of initial and final (2 600 h) characterizations.

4. Conclusion

An endurance test of 2 600 h was carried out to study the aging effects on 4 HT-PEMFC single cells with and without high frequency current ripples. The test bench used for this test is able to operate two power circuits with two cells placed in series on each circuit. The aging of two cells operated with a triangular current waveform of frequency 20 kHz and amplitude 20 %_{pp} of the mean current density (0.2 A/cm²) was compared to the aging of two cells operated at the same constant mean current density.

Despite certain events, a controlled shut-down after 1 000 h of endurance and a brutal emergency shut-down after 2 300 h of endurance, the evolution of the parameters (voltages, pressures...) during endurance and characterization phases was studied to evaluate the impact of these HFRCR on the single cells. The evolution of cells voltages during endurance is relatively similar for 2 300 h, with no difference between power circuits. The comparison of the polarization curves at initial state and after 1 000 h of endurance (intermediate characterization) shows an increase in activation losses (and diffusion to a lesser extent) for all cells, with no strong difference between the power circuits. The achieved identification of the parameters of a quasi-static model of the fuel cell for the initial and intermediate polarization curves confirm an increase in activation losses. The reduction in ECSA for all cells is confirmed by cyclic

voltammograms performed at initial state and after 2 600 h of endurance.

This paper has shown that, for the specific conditions of the test performed, no specific impact of the HFRCR on the degradation of the HT-PEMFC single cells has been identified. If confirmed by further studies, the negligible impact of HFRCR on the aging of HT-PEMFC would be an important advantage in the sizing and operation of energy systems using this fuel cell technology, allowing to reduce the size of the power converter filters and to extend the lifetime of the fuel cell. It is also found that comparing multiple components increase the robustness of the test, avoiding drawing conclusions too quickly.

Further studies are necessary to conclude more largely on the impact of HFRCR on HT-PEMFC. Such tests should include new endurance tests on cells or stacks, with less degrading and more regular characterization phases. The current waveform should be modified with variation of ripples frequency, amplitude, mean current value or operating conditions of the fuel cell. The post-mortem analysis of HT-PEMFC MEA cycled with and without the HFRCR could also be performed in addition to electrochemical characterizations. It would allow to study the impact of such harmonics on membrane and electrodes' thicknesses, acid and Pt spatial distribution in the membrane and/or in the active layer, and Pt particle size distribution.

5. Acknowledgments

The authors would like to thank Safran Power Units and the Banque Publique d'Investissement (BPI) for the financing of this work achieved in the framework of the French project PIPAA (Piles à combustible pour applications aéronautiques i.e. Fuel cells for commercial applications).

6. References

- [1] Araya SS, Zhou F, Liso V, Sahlin SL, Vang JR, Thomas S, et al. A comprehensive review of PBI-based high temperature PEM fuel cells. *International Journal of Hydrogen Energy* 2016;41:21310–44. <https://doi.org/10.1016/j.ijhydene.2016.09.024>.
- [2] Pratt JW, Klebanoff LE, Munoz-Ramos K, Akhil AA, Curgus DB, Schenkman BL. Proton exchange membrane fuel cells for electrical power generation on-board commercial airplanes. *Applied Energy* 2013;101:776–96. <https://doi.org/10.1016/j.apenergy.2012.08.003>.
- [3] Zimmermann T, Keil P, Hofmann M, Horsche MF, Pichlmaier S, Jossen A. Review of system topologies for hybrid electrical energy storage systems. *Journal of Energy Storage* 2016;8:78–90. <https://doi.org/10.1016/j.est.2016.09.006>.
- [4] Fontès G. Modélisation et caractérisation de la pile PEM pour l'étude des interactions avec les convertisseurs statiques. thesis. Toulouse, INPT, 2005.
- [5] Zhan Y, Guo Y, Zhu J, Li L, Yang B, Liang B. A review on mitigation technologies of low frequency current ripple injected into fuel cell and a case study. *International Journal of Hydrogen Energy* 2020. <https://doi.org/10.1016/j.ijhydene.2020.06.204>.
- [6] Choi W, Howze JoW, Enjeti P. Development of an equivalent circuit model of a fuel cell to evaluate the effects of inverter ripple current. *Journal of Power Sources* 2006;158:1324–32. <https://doi.org/10.1016/j.jpowsour.2005.10.038>.
- [7] Gemmen RS. Analysis for the Effect of Inverter Ripple Current on Fuel Cell Operating Condition. *Journal of Fluids Engineering* 2003;125:576–85. <https://doi.org/10.1115/1.1567307>.
- [8] Zhan Y, Guo Y, Zhu J, Liang B, Yang B. Comprehensive influences measurement and analysis of power converter low frequency current ripple on PEM fuel cell. *International Journal of Hydrogen Energy* 2019;44:31352–9. <https://doi.org/10.1016/j.ijhydene.2019.09.231>.
- [9] Kim J-H, Jang M-H, Choe J-S, Kim D-Y, Tak Y-S, Cho B-H. An Experimental Analysis of the Ripple Current Applied Variable Frequency Characteristic in a Polymer Electrolyte Membrane Fuel Cell. *Journal of Power Electronics* 2011;11:82–9. <https://doi.org/10.6113/JPE.2011.11.1.082>.
- [10] Uno M, Tanaka K. Pt/C catalyst degradation in proton exchange membrane fuel cells due to high-frequency potential cycling induced by switching power converters. *Journal of Power Sources* 2011;196:9884–9. <https://doi.org/10.1016/j.jpowsour.2011.08.030>.

- [11] Fontes G, Turpin C, Astier S, Meynard TA. Interactions Between Fuel Cells and Power Converters: Influence of Current Harmonics on a Fuel Cell Stack. *IEEE Transactions on Power Electronics* 2007;22:670–8. <https://doi.org/10.1109/TPEL.2006.890008>.
- [12] Wahdame B, Girardot L, Hissel D, Harel F, Francois X, Candusso D, et al. Impact of power converter current ripple on the durability of a fuel cell stack. 2008 IEEE International Symposium on Industrial Electronics, Cambridge, UK: IEEE; 2008, p. 1495–500. <https://doi.org/10.1109/ISIE.2008.4677206>.
- [13] Kim T, Kim H, Ha J, Kim K, Youn J, Jung J, et al. A degenerated equivalent circuit model and hybrid prediction for state-of-health (SOH) of PEM fuel cell. 2014 International Conference on Prognostics and Health Management, 2014, p. 1–7. <https://doi.org/10.1109/ICPHM.2014.7036407>.
- [14] Ma R, Xie R, Xu L, Huangfu Y, Li Y. A Hybrid Prognostic Method for PEMFC with Aging Parameter Prediction. *IEEE Trans Transp Electrific* 2021;1–1. <https://doi.org/10.1109/TTE.2021.3075531>.
- [15] Gerard M, Poirot-Crouvezier J-P, Hissel D, Péra M-C. Ripple Current Effects on PEMFC Aging Test by Experimental and Modeling. *J Fuel Cell Sci Technol* 2011;8. <https://doi.org/10.1115/1.4002467>.
- [16] Rallières O. Modélisation et caractérisation de piles à combustible et Electrolyseurs PEM. PhD Thesis. 2011.
- [17] Rastedt M, Pinar FJ, Pilinski N, Dyck A, Wagner P. Effect of Operation Strategies on Phosphoric Acid Loss in HT-PEM Fuel Cells. *ECS Trans* 2016;75:455. <https://doi.org/10.1149/07514.0455ecst>.
- [18] Jakobsen MTD, Jensen JO, Cleemann LN, Li Q. Durability Issues and Status of PBI-Based Fuel Cells. In: Li Q, Aili D, Hjuler HA, Jensen JO, editors. *High Temperature Polymer Electrolyte Membrane Fuel Cells: Approaches, Status, and Perspectives*, Cham: Springer International Publishing; 2016, p. 487–509. https://doi.org/10.1007/978-3-319-17082-4_22.
- [19] Baudy M, Rondeau O, Jaafar A, Turpin C, Abbou S, Grignon M. Voltage Readjustment Methodology According to Pressure and Temperature Applied to a High Temperature PEM Fuel Cell. *Energies* 2022;15:3031. <https://doi.org/10.3390/en15093031>.
- [20] Reiser CA, Bregoli L, Patterson TW, Yi JS, Yang JD, Perry ML, et al. A Reverse-Current Decay Mechanism for Fuel Cells. *Electrochem Solid-State Lett* 2005;8:A273. <https://doi.org/10.1149/1.1896466>.
- [21] Perry ML, Patterson T, Reiser C. Systems Strategies to Mitigate Carbon Corrosion in Fuel Cells. *ECS Transactions*, vol. 3, Cancun, Mexico: ECS; 2006, p. 783–95. <https://doi.org/10.1149/1.2356198>.
- [22] Rigal S, Turpin C, Jaafar A, Hordé T, Jollys J-B, Chadourne N. Ageing Tests at Constant Currents and Associated Modeling of High Temperature PEMFC MEAs. *Fuel Cells* 2020;20:272–84. <https://doi.org/10.1002/fuce.201900086>.
- [23] Jarry T, Lacressonnière F, Jaafar A, Turpin C, Scohy M. Modeling and Sizing of a Fuel Cell—Lithium-Ion Battery Direct Hybridization System for Aeronautical Application. *Energies* 2021;14:7655. <https://doi.org/10.3390/en14227655>.
- [24] Fontes G, Turpin C, Astier S. A Large-Signal and Dynamic Circuit Model of a H₂ O₂ PEM Fuel Cell: Description, Parameter Identification, and Exploitation. *IEEE Trans Ind Electron* 2010;57:1874–81. <https://doi.org/10.1109/TIE.2010.2044731>.
- [25] Søndergaard T, Cleemann LN, Becker H, Aili D, Steenberg T, Hjuler HA, et al. Long-term durability of HT-PEM fuel cells based on thermally cross-linked polybenzimidazole. *Journal of Power Sources* 2017;342:570–8. <https://doi.org/10.1016/j.jpowsour.2016.12.075>.
- [26] Büsselmann J, Rastedt M, Klicpera T, Reinwald K, Schmies H, Dyck A, et al. Analysis of HT-PEM MEAs' Long-Term Stabilities. *Energies* 2020;13:567. <https://doi.org/10.3390/en13030567>.
- [27] Kerr R, García HR, Rastedt M, Wagner P, Alfaro SM, Romero MT, et al. Lifetime and degradation of high temperature PEM membrane electrode assemblies. *International Journal of Hydrogen Energy* 2015;40:16860–6. <https://doi.org/10.1016/j.ijhydene.2015.07.152>.
- [28] Galbiati S, Baricci A, Casalegno A, Marchesi R. Degradation in phosphoric acid doped polymer fuel cells: A 6000 h parametric investigation. *International Journal of Hydrogen Energy* 2013;38:6469–80. <https://doi.org/10.1016/j.ijhydene.2013.03.012>.
- [29] Tognan M. Etude de dégradations des performances de Piles à Combustible PEM BT alimentées en H₂/O₂ lors de campagnes d'endurance : du suivi de l'état de santé en opération à la modélisation du vieillissement. thesis. Toulouse, INPT, 2018.
- [30] Rigal S. Etude du vieillissement et modélisation des piles à combustible PEM Hautes Températures (PEM-HT). 2019.